Int. J. Heat Mass Transfer. Vol. 16, pp. 897–916. Pergamon Press 1973. Printed in Great Britain

HEATED LAMINARIZING GAS FLOW IN A SQUARE DUCT

K. R. PERKINS, K. W. SCHADE and D. M. McELIGOT

Energy, Mass and Momentum Transfer Laboratory, Aerospace and Mechanical Engineering Department, University of Arizona, Tucson, Arizona 85721, U.S.A.

(*Received* 1 *December* 1971 *and in revised form* 6 *August* 1972)

Abstract—Experiments in a vertical, rounded-corner square duct are reported for heating rates which cause significant property variation in helium and nitrogen. New data are presented for adiabatic wall friction in laminar, transitional and turbulent flow and for heated flows in the low Reynolds number, turbulent range. The validity of an existing correlation for variable properties turbulent flow is extended down to $Re_i = 4000$. In laminar flow, effects on local heat transfer parameters are slight but local friction factors vary strongly as the wall-to-bulk temperature ratio varies. Data concentrated in the range $3000 < Re_i < 10^4$ are examined to determine heating rates which cause premature laminarization as the Reynolds number decreases axially along the tube. Laminarization criteria based on inlet conditions correspond to values of the "critical" acceleration parameter observed for two-dimensional, accelerated, external flows. Local heat transfer measurements show a wall shear stress parameter provides a better indication of incipient laminarization along the duct than the acceleration parameter.

NOMENCLATURE

A_{cs}, cross sectional area;
c_p, specific heat at constant pressure;
D_h, hydraulic diameter;
G, average mass flux, $\dot{m}/A_{cs}$;
g, gravitational acceleration;
g_c, dimensional constant;
h, convective heat transfer coefficient, $q'_w/P(T_w - T_m)$;
i, electric current;
k, thermal conductivity; surface roughness;
$\dot{m}$, mass flow rate;
P, perimeter;
p, pressure;
q'_w, heat transfer to gas per unit length;
r, corner radius;
R', electrical resistance per unit length;
T, absolute temperature;
t, wall thickness;
u, axial velocity component;
v_*, shear velocity, $\sqrt{(g_c\tau_w/\rho)}$;
V_m, gas bulk velocity;
x, axial coordinate;
y, transverse coordinate measured from wall;
y_l, viscous sublayer thickness.

Greek symbols

μ, viscosity;
ν, kinematic viscosity, μ/ρ;
ρ, density;
τ_w, apparent wall shear stress,

$$-\frac{D_h}{4}\frac{\mathrm{d}}{\mathrm{d}x}[p + G^2/\rho g_c].$$

Non-dimensional parameters

f, apparent friction factor, $2g_c\tau_w\rho/G^2$;
D_h^+, hydraulic diameter, v_*D_h/ν;
Gr_q, Grashoff number based on wall heat flux, $gD^4q''_w/(\nu^2\mu c_pT)_i$;
Gr^*, modified Grashoff number, gD_h^3/ν^2;
K, thermal acceleration parameter, $(\nu/V_m^2)\,\mathrm{d}V_m/\mathrm{d}x$;
Nu, Nusselt number, hD_h/k; Nu_{BP}, equation (11);
Pr, Prandtl number, $\mu c_p/k$;

Q^+, laminar wall heat flux parameter, $D_h q''_w/(2k_i T_i)$;
q^+, turbulent wall heat flux parameter, $q''_w/(Gc_{p,i}T_i)$;
Re, Reynolds number, GD_h/μ;
St, Stanton number, h/Gc_p;
x^+, axial distance, $2x/(D_h Re_m Pr_m)$;
Δ, wall shear stress parameter, equation (18).

Subscripts
cp, evaluated from constant property prediction;
i, inlet;
m, evaluated at local bulk temperature;
w, wall, evaluated at wall temperature.

INTRODUCTION

NON-CIRCULAR ducts are used for gas cooled nuclear power reactors, for compact heat exchangers in the process industries and for regeneratively cooled rocket nozzles. From a thermal standpoint, turbulent flow is usually desirable, but pumping power restrictions and possible failure modes force consideration of transitional and laminar flow as well. In order to conserve both space and power effectively, one must have accurate design criteria. The purpose of this investigation is to provide, by experiments, design criteria for square tube applications where the temperature-dependent properties may vary significantly.

In many applications the tubing is small. Since commercial tubing is normally employed in production, the square ducts used typically have slightly rounded corners rather than the perfectly sharp corners idealized in most analyses for non-circular tubes. As the tube size becomes smaller, the corner curvature becomes more important. Accordingly, the test section chosen for these experiments is a commercially available square tube with a corner-radius-ratio (r/D_h) of about one tenth. For most heated gas flows and many liquid flows, conduction in the duct walls usually will equalize the temperature around the periphery despite large peripheral variation of the external conditions. Thus, the appropriate analytical idealization is an isothermal periphery; this idealization is approximated in the experiments reported herein. Results for the isothermal case are further useful for comparison in determining the importance of non-isothermal effects.

Conceptually, it is possible to solve the laminar problem using a numerical approach. Such methods are now used routinely for two-dimensional boundary layer problems [1]. However, with flow readjustment due to temperature-dependent viscosity and density, the heated duct problem becomes a three-dimensional one including significant spanwise diffusion terms. Thus, numerical methods for "three-dimensional" swept wings are not applicable.

With temperature dependent properties the governing energy and momentum equations become coupled, necessitating simultaneous solution. Under the usual boundary layer approximations both equations become non-linear, parabolic partial differential equations [2]. In general, to solve such equations numerically, they are phrased in finite difference forms, in which the dependent variables at each axial location are written in terms of the known values at one or more previous locations. Since there are two significant transverse directions, this procedure becomes equivalent to solving an elliptic boundary-value problem at each axial step. Currently, computer storage and time requirements to solve two-dimensional elliptic problems in detail are extensive if not excessive. Although promising three-dimensional numerical methods are under development by Spalding and co-workers [3] and by Pierce and Klinksiek [4], it is unlikely that many design engineers will have computers, with both sufficient speed and memory, readily available to handle the three-dimensional problem effectively. Solution of the flow problem for the small commercial ducts will involve a further complication; for accuracy near the rounded corners it will probably be expeditious to introduce a finer circular grid along with the primary rectangular grid.

For variable-property flow in square ducts, numerical solution of the turbulent problem and the laminarizing problem is subject to the difficulties described above and is also hampered by insufficient knowledge of the transport mechanisms. Although several existing turbulence models give reasonable predictions in the fully turbulent regime in circular tubes, their use for the laminarizing regime yields inadequate results [5]. Accordingly, the present study emphasizes experimental measurement of heat transfer and wall friction parameters for laminar flow and laminarizing turbulent flow of strongly heated gases through square tubes. It is hoped that in the near future current turbulence research will have progressed to the point where these data can be used in the verification of a more generally valid turbulence model than is presently available.

In summary, the small duct with rounded corners is technologically important, but since the pertinent problems are not currently amenable to direct analysis it is necessary to use an experimental approach. Figure 1 summarizes the range of variables covered in the present experiment.

PREVIOUS WORK

For laminar flow, geometry has a pronounced effect on heat-transfer and friction coefficients. This fact is well documented for fully developed flow under the idealization that fluid properties are constant [6]. Montgomery and Wibulswas [7] showed further that geometry also affects the thermal entry region in rectangular ducts. Assuming constant properties and a fully developed velocity profile, they performed a numerical analysis which showed heat transfer coefficients in the thermal entry region to vary by forty percent as the aspect ratio ranged between one and four. Their results are not known to have been verified experimentally. For ethylene glycol, Hwang and Hong have considered the effect of viscosity variation in a "fully developed" analysis for laminar flow in a square duct; they also present measurements in a square tube countercurrent heat exchanger with fair agreement [8].

	Nitrogen	Helium
Experimental runs	16	12
Inlet bulk Reynolds number	3200–25400	1100–4600
Exit bulk Reynolds number	1900–16500	630–2600
Maximum T_w/T_i	3·4	3·4
Maximum T_w (°R)	1810	1820
Maximum q^+ (turbulent)	0·0040	0·0030
Maximum Q^+ (laminar)	—	2·5
Maximum Gr_q/Re_i^2 (turbulent)	$1·5 \times 10^{-3}$	$2·1 \times 10^{-5}$
Maximum Gr_i^*/Re_i (laminar), [9]	—	0·03
Maximum Mach number	0·29	0·24
Corner radius of curvature/hydraulic diameter	0·08	0·08
x/D_H for heat-transfer coefficients	3·0–109	3·0–109
x/D_H for friction factors	—	6·8–92

FIG. 1. Range of variables in the present experiment.

For gaseous laminar flow in a circular tube, Worsøe-Schmidt and Leppert [9] developed a numerical solution accounting for property variation; it is quite consistent with existing data. Their results show only a slight increase in the Nusselt number but a large increase in the friction coefficient (maximum differences of six per cent and fifty per cent, respectively, at a peak T_w/T_m of 1·5) when compared to constant property predictions in the thermal entrance region. Recent analyses for parallel plates and annuli show comparable property dependence [10, 11].

Gaseous variable property results for the square duct are apparently limited to experiment. Battista and H. C. Perkins [12] suggest that their data agree with correlations given by Campbell and H. C. Perkins [13] for a triangular duct. Their results, however, are limited to turbulent flow at inlet Reynolds numbers greater than 2×10^4. Laminar and transitional flow in a square duct was tackled by Lowdermilk, Weiland and Livingood [14] as early as 1954 but they obtained *average* parameters and, at the time, the phenomenon of laminarization was not recognized.

Laminarization—that is, apparent laminar behavior at local Reynolds numbers normally associated with turbulent flow—has been observed in strongly heated internal gas flows [15–17] and in accelerated "external" flows [18, 19]. With internal flow in the low Reynolds number range, a slight change in the heating rate can lead to a striking change from turbulent downstream behavior to laminar behavior. The consequence is a substantial reduction in local heat transfer coefficient and an increase in wall temperature. The danger is obvious. Until turbulence models are developed to predict parameters through the axial laminarization process accurately, the engineer needs design criteria to predict when it is imminent. For accelerated flows, critical laminarization parameters have been presented by both Launder [18] and Moretti and Kays [19]. By a transformation to a heating parameter, McEligot, Coon and Perkins [20] have shown that laminarization inside circular tubes can be predicted by using approximately the same value of the critical acceleration parameter as suggested by Moretti and Kays. However, whether their observation is valid for all internal flows is yet to be shown. One might expect that in non-circular ducts the proximity of adjacent walls in the corner regions would hasten laminarization. Although the rounding of the corner should lessen such an effect, the viscous sublayer is apparently thickened by strong heating so that y_l/D_h will exceed r/D_h at higher Reynolds numbers than in adiabatic flow and, consequently, the effect of adjacent walls would be felt at higher Reynolds numbers. It is difficult to predict whether the net effect will be important for the present case except by comparison to circular tube data.

THE EXPERIMENT

The equipment used was a redesigned version of the heat transfer loop employed by Reynolds, Swearingen and McEligot [21]. The essentials are illustrated in Fig. 2. Test gas (helium or nitrogen) flows from commercial gas cylinders through a series of three pressure regulators, the last being a Honeywell "Precision Pressure Regulator," to keep pressure fluctuations to a minimum. The gas passes through one of two Brooks rotameters, which are used in setting the desired flow rates, and then enters a mixing chamber where the bulk temperature is measured. This chamber leads to the entrance of a vertical test section, which is heated resistively by a.c. current from a Sorenson line voltage stabilizer, an adjustable transformer and a 20-to-1 transformer. After leaving the test section, the gas is cooled to room temperature by a countercurrent water heat exchanger so that the flow rate can be measured more accurately. It then passes through the flow control valve and into a Parkinson–Cowan Type D1 positive displacement flow meter which is specified to provide half percent accuracy at ambient conditions.

A Hewlett Packard Model 3450A digital voltmeter measures thermocouple e.m.f. Power is measured with a Fluke Model 883AB differential voltmeter in conjunction with a Weston Model 370 ammeter. Since the Fluke voltmeter is an averaging type (after rectifying to pulsating d.c.), rather than a true r.m.s. meter, harmonic distortion caused by the power supply

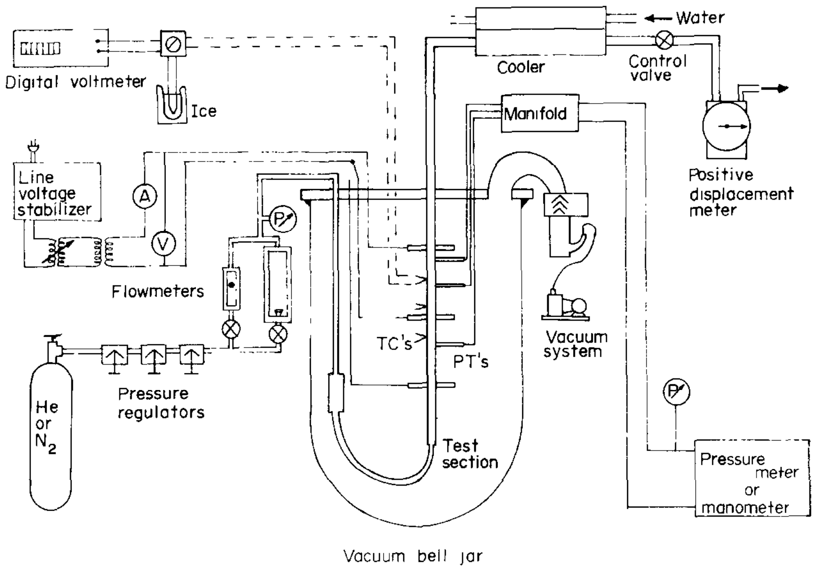

FIG. 2. Schematic diagram of experimental apparatus.

could lead to errors in the voltage measurement and resistance calculations. However, an analysis of the harmonics under load predicted that the Fluke voltmeter should be accurate to within one percent at the power levels used. Comparison to Weston Model 341 voltmeters showed that measurements with the Fluke voltmeter were within one half per cent of the true r.m.s. voltage over the entire power range. Axial pressure differences are obtained with an MKS Baratron Pressure Meter, Model 77, with 1 mm Hg (133 N/m^2) differential pressure transducer, having a sensitivity of 1×10^{-5} torr ($1{\cdot}33 \times 10^{-3}$ N/m^2), or with a Meriam micromanometer or inclined manometer, as appropriate. Pressure levels below 2 atmospheres are determined with vertical mercury or water manometers, while a Heise gage ($\pm 1{\cdot}3 \times 10^3$ N/m^2 specified accuracy) is employed for higher pressures.

A vacuum environment is provided in an inverted bell jar, 40 in. × 18 in. dia. (100 cm × 55 cm), in order to minimize heat loss effects while allowing a *localized* radiant heat loss calibration. The vacuum also reduces the response time necessary to reach steady conditions with heating.

Test section

The test section consists of a commercially available, seamless, extruded, Inconel 600 tube having a nominally square shape. From examination of metallograph pictures at 25 × magnification, it was found to have a cross-sectional area of 5·87 square mm (0·0091 square in.), a hydraulic diameter of 2·49 mm (0·098 in.), and a wall thickness of 0·38 mm (0·015 in.). The small diameter minimized the possibility of natural convection effects which otherwise could be a problem at low Reynolds numbers. The radius of curvature at the corners is approximately 0·2 mm (0·008 in.). Tubing from the same manufacturer's run was used by Battista and Perkins [12].

Of the three electrodes shown in Fig. 2 only the two upper ones were used for reported data. (The lowest electrode permits an alternate method of calibrating the middle electrode heat loss. This method was not used in the present experiment.) In the normal flow run configuration with power across the upper two electrodes, the hydrodynamic entry length is 188 hydraulic diameters and the heated section is 121 hydraulic diameters long. Thermal expansion is accommodated by supporting the test section at its upper end only and simply passing the lower, adiabatic section through a pair of Teflon guides to maintain vertical alignment.

The heat transfer surface texture is described as bright, smooth and uniform by the manufacturer. Inner surface roughness is claimed to be 125 µin. r.m.s. ($\sim 3\,\mu$). Roughness measurements with an industrial profilometer yielded an estimate of 20–30 µin. r.m.s. ($\sim \frac{1}{2}\,\mu$). However optical viewing of a fresh piece of tubing at 1000× showed roughness elements about 200 µin. ($\sim 5\,\mu$) apart and, by roughly calibrating the travel of the microscope drive, depths of 100–200 µin. With the aid of stereoscopic photographs at 700× and 7000× on a Cambridge "Stereoscan 600" scanning electron microscope, heights were found to be about 2–3 µ ($\sim$ 100 µin.). The scanning electron microscope was also used to examine a well-used sample of the test section employed by Battista and Perkins [12]; its appearance was comparable to distributed, non-uniform sand grains with the largest being of the order of 400 µin. (10 µ). The photographs are presented elsewhere [22]. Since their test section was always used for air flow at moderate to high pressures when heated, it is believed that the surface texture observed on that sample would be an upper bound on the roughness of the present test section which normally employed helium or nitrogen as the test gas. Thus, relative roughness, k/D_h, was estimated to be in the range 0·001–0·004.

Premium grade chromel–alumel thermocouples of 0·005 in. ($\sim$0·13 mm) diameter were spot welded to the test section along the centerline of one face. The so-called parallel junction —each wire separately attached—was employed; Moen showed that this method reduces the error compared to the more common crosss type junction because the effective junction is on the surface rather than partially along a fin perpendicular to the surface [23]; our past measurements have confirmed his observation. At a number of locations additional thermocouples were attached at a corner to measure the circumferential temperature variation.

Pressure tap orifices were about 5 mil ($\sim$0·13 mm) holes which were electrostatically drilled after the pressure taps were attached to obtain burr-less holes. Thus, the ratio of hole diameter to test section diameter was less than 1:10. Post-experiment dissection revealed that a slight hemispherical protuberance of radius $D_h/8$ had been formed in fabricating the pressure tap in the middle electrode. For turbulent flow, the orifice results of Krall and Sparrow [25] indicate that the effect on local Nusselt number would decay to much less than two percent by $x/D_h \approx 9$. If it is assumed that in laminar flow the effects on the mean, peripherally-averaged Nusselt number are negligible beyond three to five diameters of the protuberance, then data for $x^+ \gtrsim 0{\cdot}004$ would not be significantly disturbed.

From the reduced data, it was found that local axial heating rate to the gas could be represented approximately as a step increase, followed by a gradual decrease as the heat loss increased axially with the wall temperature. The percentage change depended on the test gas, Reynolds number and heating rate. The measured deviation from a constant peripheral outer wall temperature was found to be within 2°F (1°C) for these tests. This observation is consistent with the correlation of $(T_{\text{corner}} - T_{\text{center}})/(T_{\text{center}} - T_m)$ vs Nu/S^* developed by Lowdermilk, Weiland and Livingood [14] for predominantly turbulent flows. In the present experiment the wall conduction parameter,

$$S^* = k_{\text{wall}}t/(k_{\text{gas}}D_h) \quad (1)$$

is about 10 for helium and about 70 for nitrogen. Thus, the experimental boundary conditions approached the analytical idealization of a specified axial heating rate with locally constant temperature around the circumference.

Procedure

A number of preliminary experiments were conducted to calibrate the equipment and to insure that it was functioning properly. Of these, the initial tests were adiabatic friction measurements, which will be described later under Results.

The second group of experiments were heat loss calibrations conducted by heating the test section without internal gas flow. These runs provided data for a number of calibrations. Test section emissivity, $\varepsilon(x, T_w)$, was determined locally. In data reduction for flow runs, the local energy generation is calculated from the i^2R' product so data for the resistance calibration, $R'(T_w)$, were also obtained during the heat loss runs. Several runs of this type included internal thermocouple probe measurements to calibrate the "radiating thermocouple conduction error," i.e. the temperature depression caused by axial conduction to the wall thermocouples which act as radiating fins [25]. This error is typically 1–2 per cent of the thermocouple signal. Although the energy generation rates and boundary conditions differ between runs with flow and without flow, Hess found the effect on the thermocouple conduction error to be small provided the thermocouple conductance is large compared to the wall heat transfer coefficients [25]. For forced convection of gases the change is of the order of 10 per cent of the error, or 0·1–0·2 per cent of the signal.

Once preliminary results were obtained, a procedure evolved to obtain the data for flow with heating. First, the system was checked for leaks, thermocouple readouts were checked, and all manometers to be used were zeroed. Usually an adiabatic flow run was then conducted at the desired flow rate and comparisons were made to previous adibatic runs. If all was in order, power was applied to the test section by establishing a constant voltage setting on the adjustable transformer. When steady state was reached, measurements were taken. Since the response of the small pressure tap orifices in the test section was relatively slow, temperatures, power and flow rate were measured both before and after each set of axial pressure difference measurements to insure that the system had not suffered from some disturbance during the test.

Data were reduced at the C.D.C. 6400 computer facility of The University of Arizona. The basic computer program is described elsewhere [13, 15] and details of the modification for the vacuum environment are presented by Reynolds [26]. Discussion of the deduced parameters for non-circular ducts is provided by Campbell and Perkins [13] and their definitions are presented in the Nomenclature. Tabulated data are available from the authors at cost.

Experimental uncertainties

Laminar flow measurements pose a severe test of internal, forced convective heat transfer apparatus since per cent uncertainties for most deduced parameters increase as the Reynolds number is lowered. For the present study, uncertainty analyses based on the method of Kline and McLintock [27] were performed for a number of experimental runs. Typical estimates for the uncertainty of deduced Nusselt numbers and friction factors are listed in Fig. 3.

	Gas	Re_i	Max. q^+	Axial range	Estimated uncertainty (%)	
f	He	>1000	0·005	$0·013 < x^+ < 0·4$	7	Laminar
Nu	He	900–1400	0·005	$0·009 < x^+ < 0·2$	4	Laminar
Nu	He	1400–1800	0·004	$0·006 < x^+ < 0·15$	3	Laminar
Nu	N_2	2000–3500	0·003	$3 < x/D_h < 108$	7	Relaminarizing
Nu	N_2	3500–5500	0·004	$3 < x/D_h < 108$	7	Relaminarizing
Nu	N_2	5000–10000	0·003	$3 < x/D_h < 108$	5	Turbulent

FIG. 3. Estimated experimental uncertainties.

Heat transfer parameters are strongly dependent on the q'_w uncertainty which depends, in turn, on the ratio of the external radiative resistance to the internal convective resistance. Since the radiative resistance is a relatively fixed function of temperature, this uncertainty is primarily reduced by increasing the convective heat transfer coefficient. At a fixed Reynolds number, the Nusselt number (hD_h/k) does not vary widely as the heating rate is varied, so h may be increased by decreasing D_h and increasing k. Thus, the small size of the test section helps. For laminar flow we also found it necessary to take advantage of the higher thermal conductivity of helium compared to nitrogen. Increasing h also reduces the axial change in q'_w, so using helium actually provided a more constant axial heating rate for the laminar runs than for some turbulent data with nitrogen.

The uncertainty in duct diameter enters the friction factor calculations quite differently from the Nusselt number. Taking a sharp-cornered duct for convenience, one can see the calculations are

$$f = \frac{+g_c\rho_m D_h^5}{2\dot{m}^2}\frac{\mathrm{d}}{\mathrm{d}x}\left[p + \frac{\dot{m}^2}{g_c\rho_m D_h^5}\right] \tag{2}$$

and

$$Nu = q'_w/[4k_m(T_w - T_m)] \tag{3}$$

in terms of "measured" quantities. So the Nusselt number is not directly dependent on the uncertainty in D_h while the friction factor is strongly sensitive. Accordingly, results demonstrating the effect of property variation on wall friction will be presented in normalized form, $f\cdot Re/(f\cdot Re)_{cp}$ with $(f\cdot Re)_{cp}$ measured on the same duct, to reduce the effect of the uncertainty due to diameter measurement. When normalized, the dominant uncertainty in the friction factor is the uncertainty in pressure differences between closely spaced pressure taps.

Concerning heat transfer, axial conduction losses tended to increase the Nusselt number uncertainty significantly near the electrodes despite calibration. At the upper end of the test section $(x/D_h > 80)$, uncertainty in the Nusselt number was also increased by an increase in the percentage uncertainty of the temperature difference,

$$\frac{\delta(T_w - T_m)}{T_w - T_m} \approx \frac{\sqrt{[(T_w/T_m)^2(\delta T_w/T_w)^2 + (\delta T_m/T_m)^2]}}{(T_w/T_m) - 1} \tag{4}$$

as T_w/T_m approaches unity.

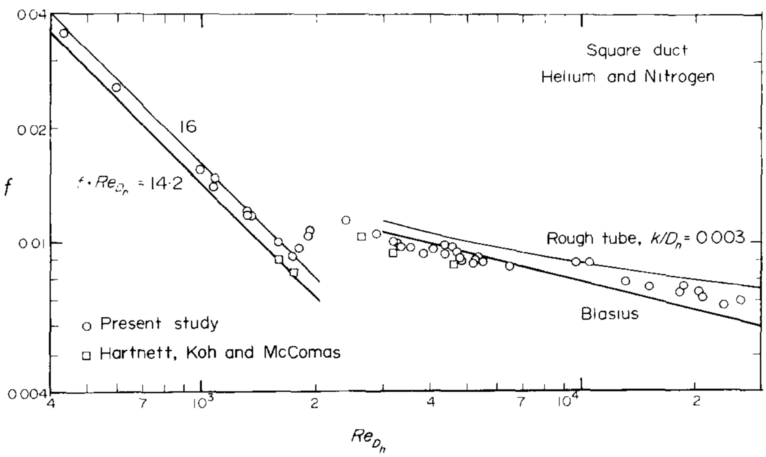

FIG. 4. Adiabatic friction measurements.

In addition to Fig. 3, estimated uncertainties are indicated by light bracketed lines on some of the figures presenting the experimental results.

RESULTS

Adiabatic flow

Throughout the period of testing, unheated flow measurements were conducted in the range $400 \lesssim Re \lesssim 30{,}000$ with helium and nitrogen. The data are presented in Fig. 4. For laminar flow in our rounded-corner square duct, these correlated as

$$(f \cdot Re)_{cp} = 15{\cdot}7 \qquad (5)$$

which is close to the analytic value for a circular tube. For a sharp-cornered square tube, one would expect $f \cdot Re = 14{\cdot}2$ [6]. Since overall pressure differences were used to calculate the friction factor, the experimental uncertainty in $(f \cdot Re)_{cp}$ is primarily dependent on the hydraulic diameter measurement which is believed to be known within one per cent. Accordingly, the uncertainty of $(f \cdot Re)_{cp}$ is estimated as about 4 per cent.

While the increased friction factor may seem surprising at first, an approximate analysis reveals that it is reasonable. The effect of rounding the corners is two-fold, First, the geometric definitions are modified with D_h being affected more than A_{cs}. For $(r/D_h) \simeq 0{\cdot}1$ the corrections are 4 per cent and 0·8 per cent, respectively. Secondly, the flow is modified. However, in a sharp corner there is a small region where the flow is approximately stagnant; if the rounding of the corner is of the same size or smaller than this region, the effect on the flow will be minimal. Comparing a rounded corner duct and a sharp one under the assumption that the velocity profiles are the same (i.e. $u \approx 0$ in some finite region of the sharp corner), one may approximate that (1) the mass flow rates are equal, and (2) the corner contribution to the total wall shear is negligible in both cases. Then the average peripheral wall shear stress becomes inversely proportional to the perimeter and, consequently, via the definitions in the Nomenclature, one finds

$$\frac{(f \cdot Re)_{\text{rounded}}}{(f \cdot Re)_{\text{sharp}}} \approx \left[1 - (4 - \pi)\frac{r^2}{L^2}\right]^2 \times \left[1 + \left(2 - \frac{\pi}{2}\right)\frac{r}{L}\right]^{-2} \qquad (6)$$

where L is the length of a side of the sharp-cornered square duct. For the present test section this result predicts an increase of about 7 per cent which is slightly less than the observed increase.

For turbulent flow at $Re \gtrsim 2 \times 10^4$, Hartnett, Koh and McComas [28] found friction measurements in square ducts agreed closely with the Blasius correlation for a circular tube provided that the Reynolds number is based on the hydraulic diameter. In this range the present measurements are slightly higher. A comparison to predictions by Moody [29] shows that the present data correspond to a relative sand grain roughness factor (k_s/D_h) of about 0·001. This value agrees with the observations of Battista and Perkins [12] with similar tubing, but is slightly smaller than expected from our microscopic examinations. For low Reynolds number turbulent flow, both the present measurements and those of Hartnett, Koh and McComas show a gradual divergence below the circular tube correlation. In this flow range the thickness of the viscous sublayer becomes significant in relation to the duct width so the proximity of the adjacent wall may serve to further reduce the turbulent transport in the corner region, thereby reducing the friction factor below that predicted on the basis of data for circular tubes.

The transition from laminar to turbulent flow is seen to begin at a Reynolds number of about 1800. This value is lower than one usually expects for a circular duct but is quite consistent with data of Hartnett, Koh and McComas for a sharp-cornered, smooth, square duct with an abrupt entrance [28]. Their data for this configuration are also presented on Fig. 4 for comparison; they lack measurements in the range $1800 \gtrsim Re \gtrsim 2600$ so their "critical" Reynolds number is apparently taken as an average of the two bounds established.

Heat transfer in laminar flow

To minimize uncertainties in the Nusselt number, all heated laminar runs were made with helium as the test gas. For these data the axial variation of q'_w was about 14 per cent or less. Results are reported in Fig. 5. For $x^+ > 0{\cdot}05$ they agree quite closely with the constant property analysis of Montgomery and Wibulswas [7] for a constant axial heating rate to gases flowing in a square duct. Downstream the variable property measurements are predicted well by the asymptotic calculations of Montgomery and Wibulswas and by the numerical solution of Clark and Kays [30] for fully established conditions under the usual constant property idealization. However, for $x^+ < 0{\cdot}05$ there is evidently an increase in the heat transfer coefficient of about 10 per cent. The slight lowering of the first data point has been explained nicely by Shumway for the comparable circular tube case [31].

The differences in the immediate thermal entry may be examined in more detail with the aid of a Leveque analysis as conducted by Worsøe-Schmidt for annuli [32]. At x^+ sufficiently small so that the thermal boundary layer thickness is much smaller than D_h, the problem may be treated as two-dimensional. In order to estimate the average peripheral Nusselt number, the wall velocity gradient is taken as the value corresponding to the average peripheral friction factor. Then one can show that, with a constant wall heat flux as the boundary condition, the Leveque solution would be given by

$$Nu \simeq 0{\cdot}652\,(f\cdot Re_{D_h})^{\frac{1}{3}}\,[2x/(D_h Re_{D_h} Pr)]^{-\frac{1}{3}}. \quad (7)$$

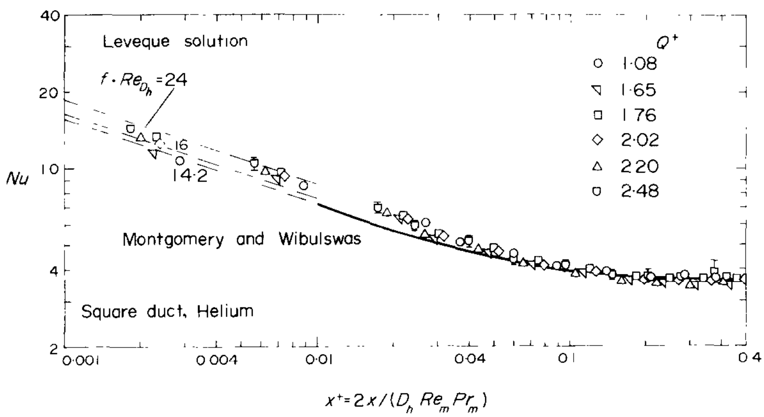

FIG. 5. Local heat transfer in laminar flow, $x/D_h \gtrsim 1$.

This prediction is plotted on Fig. 5 for the sharp-cornered square duct ($f\cdot Re_{D_h} = 14{\cdot}2$), the circular tube (16) and parallel plates (24). The numerical analysis of Montgomery and Wibulswas appears to be confirmed at $x^+ = 0{\cdot}01$, the lowest value they present.

Since the present rounded-corner test section led to adiabatic friction factors which agreed with circular tube predictions, the Nusselt number in the immediate thermal entry may be compared to the Leveque solution for $f\cdot Re_{D_h} \simeq 16$. The difference between the measurements with property variation and the constant property prediction is then about 6 per cent, which is slightly greater than the estimate of the experimental uncertainty. To put this effect into perspective, it should be noted that the fluid properties varied by up to 60 per cent across the tube in the thermal entry region.

One may conclude that for square ducts the effect of gas property variation is a slight increase of the Nusselt number in the thermal entry and a negligible effect downstream. This observation is consistent with the numerical results for symmetric circular tubes [9].

Concerning the effect of the rounded corners, it appears that for the present duct the thermal entry behavior is predicted by circular tube analyses while downstream results conform with "sharp-corner" analyses for fully established conditions with constant fluid properties. The apparent inconsistency downstream may be explained by several effects counteracting one another. An approximate analysis, based on the same assumptions as the approximate analysis for adiabatic friction factors, predicts that the Nusselt number is increased by rounding the corners,

$$\frac{Nu_{\text{rounded}}}{Nu_{\text{sharp}}} \approx \left[1 - (4-\pi)\frac{r^2}{L^2}\right] \times \left[1 - \left(2 - \frac{\pi}{2}\right)\frac{r}{L}\right]^{-2}. \quad (8)$$

Since Clark and Kays [30] used a coarse mesh with nodes spaced at $\Delta y = \Delta z = L/10$, their analysis effectively represents the same radius of curvature as the present experiment; the analysis would not discriminate between a sharp cornered duct and one with $(r/D_h) \lesssim \frac{1}{10}$ except in the calculation of A_{cs} and P in determining the Nusselt number. On the other hand, at least two effects might be expected to lead to a reduction in the Nusselt number in practise. For circular tubes, Worsøe-Schmidt and Leppert [9] predict a slight reduction in downstream heat transfer parameters under strong heating of a gas. Secondly, with resistive heating the wall boundary condition would be idealized as constant peripheral heat flux if significant conduction around the wall did not lead to an isothermal periphery; Sparrow and Siegel [33] show that the former case yields a Nusselt number about twenty per cent lower than the latter. Thus, in the experiment a slight deviation from an isothermal periphery would be expected to lead to a reduction in Nusselt number. As each of the effects considered is small and they do not all act in the same direction, it is reasonable that the downstream results agree with the numerical predictions of Clark and Kays within the estimated experimental uncertainty.

In summary, the constant property prediction of Montgomery and Wibulswas may be used for conservative design; however, their presentation is by means of a small graph which is difficult to read. Accordingly, we have correlated their results to within three per cent as

$$Nu = \left[\frac{1}{Nu_\infty} - 0{\cdot}152 \exp\{-19{\cdot}3x^+\}\right]^{-1} \quad (9)$$

for $x^+ \gtrsim 0{\cdot}015$, with Nu_∞ taken as 3·63.

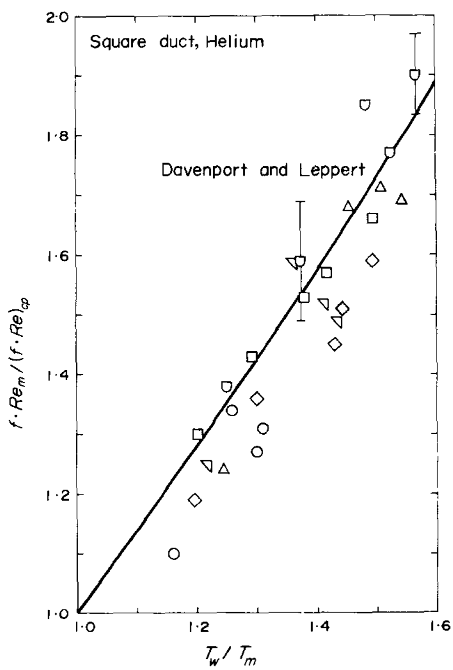

FIG. 6. Local apparent friction factor in laminar flow. Symbols as in Fig. 5.

Wall friction in laminar flow

As mentioned under Experimental Uncertainties, the effect of gas property variation has been demonstrated by normalizing the experimental friction factor results as $f \cdot Re_m/(f \cdot Re)_{cp}$ with f based on the apparent wall shear stress. Whenever possible, the value of $(f \cdot Re)_{cp}$ was taken from the adiabatic flow run preceding each heated run, in order to reduce the propagation of experimental uncertainties in flow rate and in diameter measurement. It should be noted, however, that the difference in the day-to-day results was three per cent or less.

Results are presented in Fig. 6. In contrast with the heat transfer data, there is a strong dependence on gas property variation across the duct (expressed as T_w/T_m). For comparison the correlation by Davenport and Leppert [34], for laminar flow in circular tubes,

$$(f/f_{cp}) = (T_w/T_m)^{1\cdot 35} \qquad (10)$$

is shown as well. It appears that their correlation may be extended to square ducts for design purposes, although a slightly lower exponent might be justified.

Heat transfer in turbulent flow

Since the square test section employed by Battista and Perkins [12] was a bare tube hung in atmospheric air, heat loss was greater in their experiment than in the present report. Consequently, their axial heating rate also could be described as a step change followed by a decreasing ramp function but in their worst case, at $Re \simeq 21\,000$, the variation was about 26 per cent. Their heat loss prevented them from obtaining meaningful results at lower flow rates. In contrast, the present apparatus has only an axial variation in $q'(x)$ of about 6 per cent at the same Reynolds number with nitrogen flow. Their local heat transfer results were correlated as

$$Nu_{BP} = 0\cdot021\, Re^{0\cdot8} Pr^{0\cdot4} \left(\frac{T_w}{T_m}\right)^{-0\cdot7} \times \left[1 + \left(\frac{x}{D_h}\right)^{-0\cdot7} \left(\frac{T_w}{T_m}\right)^{0\cdot7}\right] \qquad (11)$$

for the range $22 < x/D_h < 155$ and $21\,000 < Re < 49\,000$. (A printing omission occurs on the last exponent in their printed version.) The present results confirm and extend the validity of the suggested correlation.

Provided the acceleration parameter K is less than about $1{\cdot}7 \times 10^{-6}$, the present data agree with correlation (11) within 10 per cent for $12 \gtrsim x/D_h \lesssim 108$ and $4000 < Re_i < 25\,000$. For $Re_i \gtrsim 9000$ most of the data agree within 5 per cent. However, at shorter axial distances the correlation underpredicts the measured Nusselt numbers; for $x/D_h \approx 1$ the observed Nusselt number is 50–100 per cent higher.

Classification of flow regime

Any internal gas flow will become laminar if heated for a sufficient distance because the local Reynolds number will eventually be reduced to 1800—if the duct does not fail first. Further, any strongly heated internal gas flow will laminarize in the sense of Patel and Head [35]—a thickening of the viscous sublayer—but that effect is covered as standard practise in empirical and numerical relations for variable property, turbulent gas flow. It must be emphasized that we do not imply either of these situations. Instead, in our operational definition, laminarization is a process where wall parameters approach the appropriate laminar predictions at local Reynolds numbers when turbulent flow is normally expected to occur. As mentioned in the Introduction, the range where laminarization occurs can be extremely important since a sudden decrease in heat exchanger performance may occur in this region. In fact, Coon [36] reports a pair of experimental runs at identical conditions —same heating rate and flow rate—where one remained turbulent and the other evidently laminarized.

The most obvious way of testing for this condition might appear to be to insert a hot-wire anemometer into the flow. This approach would not be possible in the present apparatus without greatly altering the flow since the tube is only about 2·5 mm (0·1 in.) wide. More importantly, turbulence level measurements may not show when viscous effects dominate despite turbulent fluctuations and, in turn, lead to wall parameters which agree with laminar predictions. In a separate, unpublished experiment with a larger, circular tube at The University of Arizona, R. J. Pederson found that oscilloscope traces from a hot wire anemometer apparently showed normal turbulent flow although wall parameters indicated that laminarization had taken place.

A number of wall parameters can serve as indicators of laminarization. Bankston [16] has demonstrated that local Stanton number measurements can give a clear indication of whether laminarization occurs; Fig. 7 is an example. Several runs are plotted for two enter-

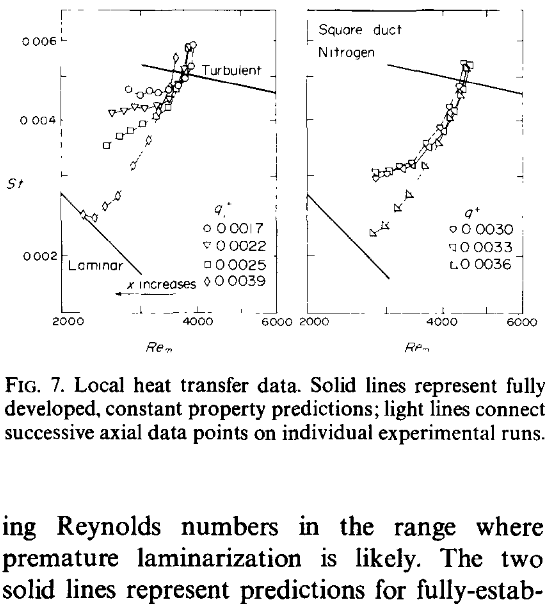

FIG. 7. Local heat transfer data. Solid lines represent fully developed, constant property predictions; light lines connect successive axial data points on individual experimental runs.

ing Reynolds numbers in the range where premature laminarization is likely. The two solid lines represent predictions for fully-established laminar and turbulent conditions and, thus, serve as useful references. When plotted against local Reynolds number (GD_h/μ) in this fashion successive axial measurements proceed from right to left because the local viscosity increases axially.

Figure 7 is useful for identifying turbulent runs since they appear to revert to the constant properties turbulent behavior as they proceed downstream and their temperature ratio approaches unity. The data for $q_i^+ = 0{\cdot}0017$ provide an example which agrees with the turbulent variable properties correlation of Battista and Perkins [12] within ten per cent at $Re \approx 3000$. Some authorities [36] require that the data agree with the *fully developed* laminar prediction within the length of their test section in order to earn the label, laminarizing. In contrast, the *St–Re* plot clearly demonstrates conditions such as the run at $q_i^+ = 0{\cdot}0036$, where the flow has evidently laminarized prematurely (at $Re > 3000$) but will not agree with the fully-developed prediction within the duct. (The reader is reminded that laminar thermal entry lengths increase with Reynolds number and would be about 150 diameters at $Re = 3000$ [6].) The data for $q^+ = 0{\cdot}0025$ appear to be in the same category but would not reach the fully-developed prediction until $Re \approx 2000$. On the other hand, there are a number of "undetermined" runs (e.g. $q_i^+ = 0{\cdot}0030$ and $0{\cdot}0033$) for which it is not evident whether they will revert to turbulent results or whether they have laminarized prematurely.

Having established confidence in the heat transfer data in turbulent flow with $Re > 10^4$ and in laminar flow, we conducted additional heated flow runs in the laminarization regime of McEligot, Coon and Perkins [20] to determine criteria for square ducts. From examination of the data plotted on *St–Re* planes as in Fig. 7, from comparison to the correlation of Battista and Perkins [12] and from examination on the Nu–x^+ plane, runs were classified as either turbulent, laminarizing or undetermined. Results are plotted in Fig. 8. This presentation may be interpreted as showing the relationship between inlet conditions and boundary conditions which will cause laminarization when the heating is at an approximately constant axial rate. The data agree qualitatively with the classification of McEligot, Coon and Perkins. However, by concentrating more experimental runs in their transitional range, the uncertainty in the laminarization criterion has been reduced for the present square tube.

Alternatively, the data could be plotted using a suitably defined acceleration parameter instead of the heat flux parameter shown. However, as McEligot, Coon and Perkins have shown, the two approaches are closely related. In particular, for low Mach number flow of a strongly heated perfect gas, one can show that the acceleration parameter is related to the heat flux parameter as

$$K_i = \frac{\nu}{V_m^2} \frac{dV_m}{dx}\bigg|_i \approx \frac{4q^+}{Re_{D_h,i}} \tag{12}$$

for any uniformly heated duct of arbitrary shape. With these approximations, the critical acceleration factor suggested by Coon [36] for a circular tube has also been plotted in Fig. 8.

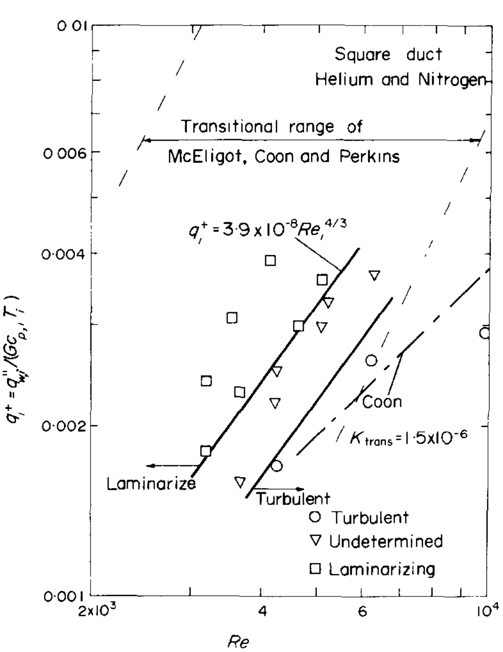

FIG. 8. Flow regime classification for square duct.

The question—of whether adjacent walls significantly increase the Reynolds number at which laminarization of a turbulent flow occurs—is answered. They evidently do not. While the viscous sublayer is likely thickened by strong heating (as shown by numerical predictions which account for property variation), it appears that it is not thickened enough in this range to interfere with the hydraulic diameter analogy—which depends on the thermal resistance being concentrated near the wall.

Coon's correlation apparently predicts laminarization at higher Re in a circular tube than the present data do for a square duct. However, the difference primarily lies in the methods of evaluating the parameters. Coon evaluated K near the exit of his tube ($x/D \approx 90$)—after his Nusselt numbers began to agree with the prediction for fully-developed, laminar flow. Since it is not clear at what axial station viscous effects become dominant, the present classification interprets the criterion as that set of conditions (i.e. K_i or q_i^+ and Re) which will cause laminarization. Accordingly, we evaluate K_i near the start of heating. Coon's figures show that K decreased by a factor of two along the tube in some of his transitional and laminar runs. Thus, if his acceleration parameter were calculated in the same manner as the present study, the agreement would be closer.

For the range of data shown on Fig. 8, we may take the separation between those runs which are undetermined and those which laminarize as a criterion for laminarization. This locus may be correlated as

$$q_{i,\,\text{trans}}^+ \approx 3{\cdot}9 \times 10^{-8}\, Re_i^{\frac{4}{3}} \tag{13}$$

as shown on Fig. 8. Alternatively, this correlation could be phrased

$$K_{i,\,\text{trans}} \simeq 1{\cdot}6 \times 10^{-7}\, Re_i^{\frac{1}{3}}. \tag{14}$$

At $Re_i = 4000$, we then have $K_{i,\,\text{trans}} \simeq 2{\cdot}6 \times 10^{-6}$ which falls between the values suggested by Moretti and Kays [19] and by Back and Seban [37] for external flows. If divergence from the turbulent correlation is preferred as a criterion, the necessary heating rate $q_{i,\,\text{trans}}^+$ would be lower, e.g. about 35 per cent lower for a 15 per cent divergence as shown by our other locus on the figure.

Local behavior during laminarization

In the previous section inlet criteria were determined for conditions leading to premature laminarization under an approximately constant wall heating rate, i.e. the situation in the present experiment. In many practical applications the heat flux varies considerably in the axial direction so the local behaviour and local criteria become important. Further, the designer is interested in knowing when the laminarizing run diverges from turbulent predictions, how the heat transfer parameters vary during the turbulent-to-laminar transition process and when the wall parameters exhibit laminar behavior.

A series of parameters are plotted in Fig. 9 for typical runs to demonstrate the local behavior. The runs have been chosen for two groupings of inlet Reynolds numbers, $Re_i \approx 4000$ and 5000, each with increasing heating rates for comparison. The same runs have been presented previously in the *St–Re* plane in Fig. 7. Each of the three flow regimes is represented.

Examining the immediate thermal entry on the sub-figures of Nu vs x^+, one sees that at a given entering Reynolds number the data converge towards a Leveque approximation, i.e. $Nu \sim (x^+)^{-\frac{1}{3}}$, regardless of heating rate. The same trend has been demonstrated previously for turbulent flow in circular tubes by the numerical analyses of Bankston and McEligot [38]. In contrast, laminar flow predictions show a distinct dependence on heating rate in the immediate thermal entry [9]. As one might expect the Leveque "asymptote" is slightly higher for the higher inlet Reynolds number; equation (7) suggests variation as $(f \cdot Re)^{\frac{1}{3}}$. However, the measured asymptotes in Fig. 9 are approximately twenty per cent higher than predicted by equation (7). Normally, the validity of a Leveque approximation is estimated to be to $x^+ \approx 0{\cdot}01$, but in these data the higher heating rate runs diverge towards a laminar prediction (for constant properties and constant q''_w, represented by solid line) somewhat earlier.

From the success in correlating flow regime

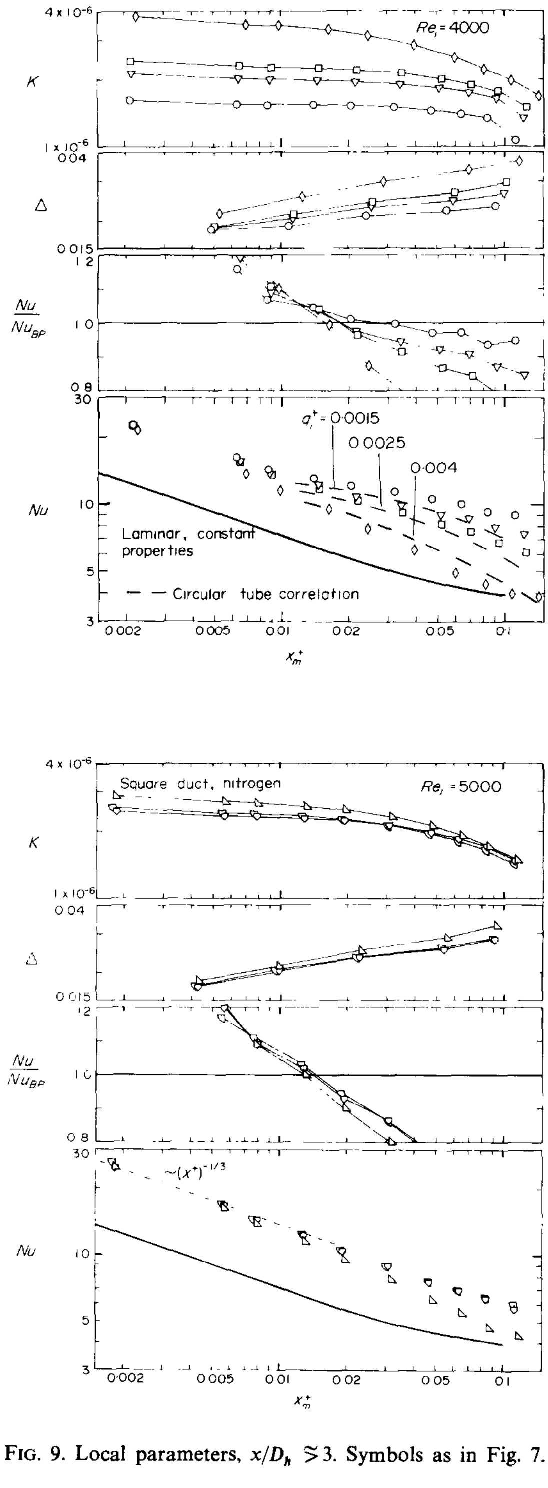

FIG. 9. Local parameters, $x/D_h \gtrsim 3$. Symbols as in Fig. 7.

by the value of the inlet acceleration parameter, it might be inferred that the flow laminarizes immediately in the thermal entry region. Since the turbulent profile in the adiabatic entry is rather blunt, even at low Reynolds numbers, one could then suggest that a solution for laminar flow with a uniform inlet velocity profile would provide reasonable predictions for the axial variation of laminarizing flows. The agreement with turbulent Leveque behavior refutes this suggestion. Further, the solution for a uniform inlet velocity profile in a circular tube [38] underpredicts the data of Fig. 9 by up to 25 per cent and the comparable solution for a square tube would be expected to be slightly lower.

In the first report of laminarizing flow due to heating [15], one of the authors developed an empiricial correlation for heat transfer during the axial transition from turbulent to laminar flow in circular tubes,

$$Nu = 0{\cdot}021\, Re_i^{-1{\cdot}2}\, Pr^{0{\cdot}4}\, Re_m^2. \tag{15}$$

This relationship was developed from data for gas entering at room temperature, as in the present experiment, and for $15 < x/D \gtrsim 100$ but the bulk of the data was concentrated below $x/D \approx 50$. If Pr, c_p and q''_w are approximated as constant, this correlation may be transformed to

$$Nu \approx 0{\cdot}021\, Re_i^{0{\cdot}8}\, Pr^{0{\cdot}4}[1 + K_i Re_i x/D_h]^{-2n} \tag{16}$$

where n represents the exponent in a power law approximation of the viscosity–temperature relationship. Alternatively, the second term in brackets may be written as $4q_i^+ x/D_h$. The correlation predicts that at a given axial location the Nusselt number will be reduced as the acceleration parameter is increased. To examine its validity for the present square test section equation (16) is plotted as dashed curves on Fig. 9a for three heating rates in the range of interest. For the experimental runs which do not agree with the turbulent correlation of Battista and Perkins [12] the trends are predicted well and the magnitudes are reasonable. Obviously, equation (16) should not be used beyond the range of conditions for which it was developed; in particular, ridiculous values would be calculated at axial distances that are either too short or too long. Agreement appears fair in the developing region beyond the immediate thermal entry.

We now attempt to develop local criteria for incipient laminarization. As a first step we estimate the location where the flow begins to laminarize. Figure 9 shows that laminarization is a gradual process rather than an abrupt change. Thus, determining the location where laminarization starts becomes a subjective process. Two of the subfigures, Nu vs x^+ and Nu/Nu_{BP} vs x^+, aid in estimating this position, or an upper bound, for each particular run. The latter subfigure provides a comparison to the turbulent, variable properties correlation of Battista and Perkins [12]. If one arbitrarily selects a criterion that laminarization has begun when the Nusselt number is 10 per cent below their prediction, then for the run* at $q_i^+ = 0{\cdot}0022$ laminarization is initiated before $x^+ \gtrsim 0{\cdot}08$. For the data at $q_i^+ = 0{\cdot}0025$ the position is $x^+ \gtrsim 0{\cdot}04$, while the $q_i^+ = 0{\cdot}0017$ run remains turbulent. Such a criterion does not appear useful for the other four runs since they show no tendency to agree with the turbulent correlation and merely cross it in the immediate entry region. Study of the Nu–x^+ trace provides limited guidance for these runs. For high Reynolds number, turbulent gas flow in circular tubes with variable properties, numerical analyses show the Nusselt number to diverge *above* the Leveque slope of $x^{-\frac{1}{3}}$ as x increases (e.g. see Fig. 8 of [38]). If the same behavior carries over to square tubes, we might infer that data which agree with the Leveque behavior beyond $x^+ \approx 0{\cdot}01$ or $0{\cdot}02$ have already begun to laminarize. Thus, for the data at $q_i^+ = 0{\cdot}0030$

* The heating rate is being used here only as a convenient identifier of a particular experimental run. Figure 6 shows that whether a run at a specific heating rate laminarizes prematurely depends also on the Reynolds number.

and 0·0033 the estimated position is $x^+ \gtrsim 0{\cdot}01$. Since the runs at $q_i^+ = 0{\cdot}0036$ and $0{\cdot}0030$ diverge *below* the Leveque behavior, we estimate that their laminarization is initiated at $x^+ \gtrsim 0{\cdot}08$ and $x^+ \gtrsim 0{\cdot}06$, respectively.

Bankston [16] demonstrated that the acceleration parameter, K, is not a useful local criterion for laminarization in circular tubes. The upper section of Fig. 9 confirms that his observation is valid for square ducts as well. From reports of external boundary layers, we expect an increased laminarizing tendency as K increases, but with internal heating with an axially constant wall heat flux, K decreases continually. The axial rate of decrease of K indicates whether laminarization is occurring since $|dK/dx|$ is greater for laminarizing flow than turbulent flow, but that is a consequence rather than a useful predictor.

Bankston [16] suggests that a pressure-gradient parameter

$$\Delta_p = -(\nu/\rho v_*^3)\,dp/dx \tag{17}$$

shows the proper trends to use as a local criterion (the sign has been changed by the present authors for convenience). Assuming acceleration is negligible compared to the pressure gradient, he converts Δ_p to

$$\Delta = \frac{4\mu_w}{D_h\sqrt{(\rho_w g_c \tau_w)}}. \tag{18}$$

For the present data neglect of the acceleration term could represent up to a 30–40 per cent error in evaluation of Δ_p, so it is best to refer to Δ simply as a "wall shear stress parameter." Further inspection shows this parameter simply to be

$$\Delta = 4/D_h^+ \tag{19}$$

where D_h^+ is the hydraulic diameter made dimensionless in "law-of-the-wall" coordinates. For a circular tube, $\Delta = 2/y_{\mathfrak{C}}^+$ which is of the order of 0·02 at $Re \approx 3000$ in adiabatic flow.

The second set of sub-figures in Fig. 9 presents the axial variation of Δ for the runs being considered and it is seen that this parameter increases as laminarization becomes more likely. The turbulent run at $q_i^+ = 0{\cdot}0017$ does not exceed $\Delta = 0{\cdot}023$. For the other runs, the axial locations determined above correspond to a range $0{\cdot}0022 \gtrsim \Delta \gtrsim 0{\cdot}025$. The lower value represents the highest heating rate; since this run readjusted most rapidly in the flow direction, it appears that the "history" of the flow is important and therefore a unique local value of Δ is not appropriate as a criterion. Since the manner in which this range was determined was to identify limiting positions where laminarization was barely discernable but was in process, a lower value of Δ should be chosen to avoid laminarization. For design purposes, Δ can be predicted locally via empirical correlations for the Nusselt number and the friction factor in variable property, turbulent flow (since only the square root of τ_w is involved, the dependence on friction factor is less sensitive) and incipient laminarization should be avoided by keeping Δ sufficiently low.

The question of how far downstream a flow must progress before results agree with laminar parameters does not have a simple answer because the family of solutions for an incompletely developed laminar flow is unknown. Also laminar predictions are sensitive to the axial wall heat flux distribution so a distance correlation determined for constant q_w'' would not necessarily be significant for a heat flux distribution encountered in a design problem. In Fig. 9 the two runs which converge closely to the laminar downstream prediction do so when $\Delta \approx 0{\cdot}035$ but there is no information available to determine whether they agreed with the appropriate (unknown) developing laminar solutions at shorter axial distances, hence at lower Δ.

CONCLUSIONS

This investigation indicates that the numerical analysis of Montgomery and Wibulswas [7], for heat transfer to laminar flow in sharp-cornered square ducts with constant properties, is substantially correct. For a duct with rounded corners instead, the peripheral average Nusselt number is slightly higher in the thermal entry.

Gas property variation affects the Nusselt number only slightly; the effect on the friction factor was found to be much greater than on the heat transfer parameters, and the correlation of Davenport and Leppert [34] for round tubes is recommended for square ducts as well.

In laminar flow, adiabatic friction factors are slightly higher than for a sharp-cornered duct and are approximately predicted by equation (6). Transition to turbulent flow occurs near $Re = 1800$.

The correlation of Battista and Perkins [12] for turbulent flow with property variation has been extended into the low Reynolds number range to $Re_i \approx 4000$ provided the acceleration parameter, K_i, is less than $1{\cdot}7 \times 10^{-6}$.

With a thermal boundary condition of a slightly decreasing wall heat flux in the range $0{\cdot}0015 < q''_w/(Gc_{pi}T_i) < 0{\cdot}004$, the criterion for premature laminarization in a square duct may be approximated by equation (13). The values represented by this result are in agreement with criteria established for laminarization of accelerated, external turbulent boundary layers.

Local heat transfer parameters for laminarizing and laminarescent runs show Leveque behavior in the immediate thermal entry, and in the developing region they are in fair agreement with an earlier correlation for circular tubes by McEligot [15]. The local value of the acceleration parameter, K, is not a useful indicator of incipient laminarization. A wall shear stress parameter, $\Delta = 4/D_h^+ = 4\mu_w/(D_h\sqrt{\rho_w \tau_w})$, appears to provide a better local criterion. Incipient laminarization is indicated when a value of Δ of the order of 0·02 is exceeded.

ACKNOWLEDGMENTS

The authors wish to acknowledge the financial support contributed by the U.S. Army Mobility Research and Development Center at Fort Belvoir and the U.S. Army Research Office, Durham. Thanks are also due to Dr. R. W. Shumway, Messrs. E. Ek and G. Hasen, and one of the referees for their valuable assistance.

REFERENCES

1. K. W. SCHADE and D. M. McELIGOT, Cartesian Graetz problems with air property variation, *Int. J. Heat Mass Transfer* **14**, 653–666 (1971).
2. G. D. SMITH, *Numerical Solution of Partial Differential Equations*. Oxford, London (1965).
3. L. S. CARETTO, R. M. CURR and D. B. SPALDING, Two numerical methods for three-dimensional boundary layers, Tech. Rept. EF/TN/A/40, Imperial College (1971).
4. F. J. PIERCE and W. F. KLINKSIEK, An implicit numerical solution of the turbulent three-dimensional incompressible boundary layer equations, Tech. Rept. VPI-E-71-14, Virginia Polytechnic Institute (1971).
5. D. M. McELIGOT and C. A. BANKSTON, Numerical predictions for circular tube laminarization by heating, ASME paper 69-HT-52, National Heat Transfer Conference (1969).
6. W. M. KAYS, *Convective Heat and Mass Transfer*. McGraw-Hill, New York (1966).
7. S. R. MONTGOMERY and P. WIBULSWAS, Laminar flow heat transfer in ducts of rectangular cross section, Proc. Third Intl. Heat Transfer Conf., Vol. 1, 107–112 (1966).
8. S. T. HWANG and S. W. HONG, Effect of variable viscosity on laminar heat transfer in a rectangular duct, A.I.Ch.E. paper 8, Natl. Heat Transfer Conf., Minneapolis (1969).
9. P. M. WORSOE-SCHMIDT and G. LEPPERT, Heat transfer and friction for laminar flow of a gas in a circular tube at high heating rate, *Int. J. Heat Mass Transfer* **8**, 1281–1301 (1965).
10. T. B. SWEARINGEN and D. M. McELIGOT, Internal laminar heat transfer with gas property variation, *J. Heat Transfer* **93**, 432–440 (1971).
11. R. W. SHUMWAY and D. M. McELIGOT, Laminar gas flow in annuli with property variation, *Nucl. Sci. Engng* **46**, 394–407 (1971).
12. E. BATTISTA and H. C. PERKINS, Turbulent heat and momentum transfer in a square duct with moderate property variation, *Int. J. Heat Mass Transfer* **13**, 1063 (1970).
13. D. A. CAMPBELL and H. C. PERKINS, Variable property turbulent heat and momentum transfer for air in a vertical rounded corner triangular duct, *Int. J. Heat Mass Transfer* **11**, 1003–1012 (1968).
14. W. H. LOWDERMILK, W. F. WEILAND and J. N. B. LIVINGOOD, Measurements of heat transfer and friction coefficient for flow of air in non-circular ducts at high surface temperature, NACA RM E53J07 (1954).
15. D. M. McELIGOT, The effect of large temperature gradients on turbulent flow of gases in the downstream regions of tubes, Ph.D. thesis, Stanford Univ., TID-19446 (1963).
16. C. A. BANKSTON, The transition from turbulent to laminar gas flow in a heated pipe, *J. Heat Transfer* **92**, 569–579 (1970).
17. C. W. COON and H. C. PERKINS, Transition from the turbulent to the laminar regime for internal convective flow with large property variations, *J. Heat Transfer* **92**, 506–512 (1970).

18. B. E. LAUNDER, Laminarization of the turbulent boundary layer in a severe acceleration, *J. Appl. Mech.* **31**, 707–708 (1964).
19. P. M. MORETTI and W. M. KAYS, Heat transfer through an incompressible turbulent boundary layer with varying freestream velocity and varying surface temperature —an experimental study, *Int. J. Heat Mass Transfer* **8**, 1187–1202 (1965).
20. D. M. MCELIGOT, C. W. COON and H. C. PERKINS, Relaminarization in tubes, *Int. J. Heat Mass Transfer* **13**, 431–433 (1970).
21. H. C. REYNOLDS, T. B. SWEARINGEN and D. M. MCELIGOT, Thermal entry for low Reynolds number turbulent flow, *J. Basic Engng* **91**, 87–94 (1969).
22. K. R. PERKINS and D. M. MCELIGOT, Roughness of heat transfer surfaces, *Int. J. Heat Mass Transfer* **16**, 679 (1973).
23. W. K. MOEN, Surface temperature measurement, *Inst. Control Syst.*, **33**, 70–73 (1960).
24. K. M. KRALL and E. M. SPARROW, Turbulent heat transfer in the separated, reattached, and redevelopment regions of a circular tube, *J. Heat Transfer* **88**, 131 (1966).
25. W. G. HESS, Thermocouple conduction error with radiation heat loss, M.S.E. thesis, Univ. of Arizona (1965).
26. H. C. REYNOLDS, Internal low Reynolds number turbulent heat transfer, Ph.D. thesis, Univ. of Arizona, DDC AD 669 254 (1968).
27. S. J. KLINE and F. A. MCLINTOCK, The description of uncertainties in single sample experiments, *Mech. Engng* **75**, 38 (1953).
28. J. P. HARTNETT, J. C. Y. KOH and S. T. MCCOMAS, A comparison of predicted and measured friction factors for turbulent flow through rectangular ducts, *J. Heat Transfer* **84**, 82 (1962).
29. L. F. MOODY, Friction factors for pipe flow, *Trans. Am. Soc. Mech. Engrs* **66**, 671 (1944).
30. S. H. CLARK and W. M. KAYS, Laminar flow forced convection in rectangular tubes, *Trans. Am. Soc. Mech. Engrs* **75**, 859–866 (1953).
31. R. W. SHUMWAY, Variable properties laminar gas flow heat transfer and pressure drop in annuli, Ph.D. thesis, Univ. of Arizona, DDC AD 696 458 (1969).
32. P. M. WORSØE SCHMIDT, Heat transfer in the thermal entrance region of circular tubes and annular passages with fully developed laminar flow, *Int. J. Heat Mass Transfer* **10**, 541–551 (1967).
33. E. M. SPARROW and R. SIEGEL, A variational method for fully developed laminar heat transfer in ducts, *J. Heat Transfer* **81**, 157–167 (1959).
34. M. E. DAVENPORT and G. LEPPERT, The effects of transverse temperature gradients on the heat transfer and friction for laminar flow of gases, *J. Heat Transfer* **87**, 191–196 (1965).
35. V. C. PATEL and M. R. HEAD, Reversion of turbulent to laminar flow, *J. Fluid Mech.* **34**, 371–392 (1968).
36. C. W. COON, The transition from the turbulent to the laminar regime for internal convective flow with large property variations, Ph.D. thesis, Univ. of Arizona (1968).
37. L. H. BACK and R. A. SEBAN, Flow and heat transfer in a turbulent boundary layer with large acceleration parameter, *Heat Transfer and Fluid Mechanics Institute* (1967).
38. C. A. BANKSTON and D. M. MCELIGOT, Turbulent and laminar heat transfer to gases with varying properties in the entry region of circular ducts, *Int. J. Heat Mass Transfer* **13**, 319–344 (1970).

ECOULEMENT D'UN GAZ CHAUFFE AVEC LAMINARISATION DANS UN CONDUIT CARRE

Résumé—Des expériences dans un conduit vertical carré avec coins arrondis sont menées pour des flux chauffants qui provoquent une variation marquée de propriété dans l'hélium et l'azote. Des nouveaux résultats sont présentés pour un frottement pariétal adiabatique dans un écoulement de transition, laminaire et turbulent et pour des écoulements chauffés dans le domaine des faibles nombres de Reynolds. La validité d'une relation existant pour un écoulement turbulent à propriétés variables est étendue à Re_i = 4000. Dans l'écoulement laminaire, les effets sur les paramètres locaux de transfert thermique sont légers, mais les coefficients locaux de frottement varient fortement avec le rapport température pariétale/température moyenne de mélange. Des résultats appartenant au domaine $3{\cdot}10^3 < Re_i < 10^4$ sont examinés afin de déterminer les flux thermiques qui sont la cause d'une laminarisation prématurée quand le nombre de Reynolds décroît axialement le long de tube. Les critères de laminarisation basés sur les conditions à l'entrée correspondent aux valeurs du paramètre d'accélération "critique" observé pour des écoulements externes bidimensionnels et accélérés. Des mesures de transfert thermique local montrent qu'un paramètre de contrainte tangentielle pariétale donne, sur la laminarisation naissante le long du conduit, une meilleure indication que le paramètre d'accélération.

BEHEIZTE LAMINARE GASSTRÖMUNG IN EINEM QUADRATISCHEN KANAL

Zusammenfassung—Es wird über Experimente mit Gasströmungen in vertikalen, quadratischen Kanälen mit abgerundeten Ecken berichtet mit Heizungsraten die zu deutlichen Änderungen der Stoffgrössen bei Helium und Sauerstoff führen. Neue Messwerte werden dargeboten für den Fall adiabater Wandreibung in laminarer und turbulenter Strömung und im Ubergangsbereich zwischen diesen beiden, sowie für beheizte Strömung bei kleinen Reynolds-Zahlen im turbulenten Bereich. Die Gültigkeit einer existierenden Korrelation bei veränderlichen Stoffwerten in turbulenter Strömung wird bis zu $Re_i = 4000$ ausgedehnt. Bei laminarer Strömung sind die Effekte durch Änderung der lokalen Wärmeübertragungsparameter klein, aber der lokale Reibungsfaktor ändert sich stark, wenn das Verhältnis der Wand- zur mittleren Flüssigkeits-Temperatur sich ändert. Die Messwerte, die im wesentlichen im Bereich $3000 < Re_i < 10^4$ lagen, wurden auf einen Heizungsparameter hin untersucht der die vorzeitige Laminarisierung der Strömung bei abnehmenden Reynolds-Zahlen entlang der Achse des Kanals erklärt.

Laminarisierungs-Kriterien die auf den Einlaufbedingungen basieren, stimmen überein mit den Grössen der "kritischen" Beschleunigungs-Parameter die an zweidimensionalen, beschleunigten Umströmungen beobachtet wurden.

Lokale Wärmeübergangsmessungen zeigen, dass ein Wand-Schubspannungs-Parameter die beginnende Laminarisierung entlang des Kanals besser wiedergibt, als der Beschleunigungsparameter.

ЛАМИНАРНОЕ ТЕЧЕНИЕ НАГРЕТОГО ГАЗА В КАНАЛЕ КВАДРАТНОГО СЕЧЕНИЯ

Аннотация—Описываются эксперименты в вертикальном канале квадратного сечения с закругленными углами при скоростях нагрева, вызывающих значительное изменение свойств гелия и азота. Представлены новые данные по трению на адиабатической стенке в ламинарном переходном и турбулентном потоках и в нагреваемых потоках при малых значениях числа Рейнольдса при турбулентном течении. Границы применимости существующей корреляции для турбулентного потока с переменными свойствами расширены до $Re_i = 4000$. В случае ламинарного течения параметры локального теплообмена претерпевают незначительное изменение, в то время как коэффициенты локального трения изменяются очень сильно по мере изменения отношения температуры стенки к среднемассовой температуре газа. Исследовались данные, относящиеся к диапазону $3000 < Re_i < 10^4$ для определения скоростей нагрева, при которых возникает преждевременная ламинаризация с уменьшением значений числа Рейнольдса вдоль оси трубы. Критерии ламинаризации, определяемые по условиям на входе, соответствуют значениям параметра критического ускорения, наблюдаемого в случае двумерных ускоренных внешних потоков. Результаты измерений локального теплообмена показывают, что параметр напряжения сдвига на стенке лучше определяет начинающуюся ламинаризацию вдоль канала по сравнению с параметром ускорения.